

Correlation between EPR, dielectric spectroscopic and conductivity studies of lithium substituted $\text{Na}_2\text{Ti}_3\text{O}_7$ ceramic

D Pal, R P Tandon* & Shripal

Department of Physics, P P N P G College, Kanpur 208 001

*Department of Physics and Astrophysics, Delhi University, Delhi 110 007

Received 31 January 2006; revised 28 March 2006; accepted 17 April 2006

The lithium substituted $\text{Na}_2\text{Ti}_3\text{O}_7$ ceramics with a general formula $(\text{Na}_{2-x}\text{Li}_x\text{Ti}_3\text{O}_7)$ with $(x = 0.1)$ have been synthesized by high temperature solid-state reaction technique. Preliminary EPR analysis and detailed temperature and variable frequency dielectric, conductivity measurements were carried out on the prepared sample. The lithium ions are accommodated with the sodium ions in the interlayer space. The EPR spectrum of $\text{Na}_{1.9}\text{Li}_{0.1}\text{Ti}_3\text{O}_7$ confirms the partial reduction of Ti^{4+} ions to Ti^{3+} . The observed dispersion in the dielectric constant-temperature relation can be explained on the basis of Maxwell-Wagner model. The conductivity plots between $\ln(\sigma T)$ versus $1000/T$ have been divided into four regions. The various conduction mechanisms in the different regions have been stressed in this paper. The interlayer ionic conduction seems to play major role in conduction towards higher temperature.

Keywords: Sintering, Dielectric properties, Ionic conductivity, TiO_2

IPC Code: G01R27/26

1 Introduction

The layered compounds show highly isotropic structural and elastic properties. They are characterized by rather rigid layers, loosely stacked together perpendicular to each other and can be intercalated with other chemical species¹. Trititanates nanotubes made by single alkali treatment². The crystal structure of more than ten sodium titanates were established while the $\text{Na}_2\text{Ti}_3\text{O}_7$ phase was among the first to be synthesized and structurally studied³. Electrical studies in some alkali titanates have been reported by Shripal *et al*⁴. The sodium titanates Na_4TiO_4 α , β -, and γ - Na_2TiO_3 , $\text{Na}_8\text{Ti}_5\text{O}_{14}$, $\text{Na}_2\text{Ti}_3\text{O}_7$ and $\text{Na}_2\text{Ti}_6\text{O}_{13}$, all of which can be synthesized in the temperature range 800-1200°C have been characterized by X-ray diffraction (XRD) and Raman spectroscopy⁵. The phase composition of $\text{Na}_x\text{M}_x\text{Ti}_{8-x}\text{O}_{16}$ ($M=\text{Al}, \text{Ga}, \text{In}$) materials was studied by X-ray diffraction⁶. A total of about 130 phases (mostly non-stoichiometric), including a dozen of sodium titanates⁷⁻¹⁵ are known. Recently, the crystal structure of $\text{Na}_2\text{Ti}_3\text{O}_7$ has been refined by Yakubovich and Kireev¹⁶. Shripal *et al*⁴ have reported the dielectric-spectroscopic and *ac* conductivity studies of pure and manganese^{17,18} doped $\text{Na}_2\text{Ti}_3\text{O}_7$. Since orbital overlap is crucial for electrical conduction, it is

important to take into consideration the joining nature of the octahedral. In case of the layered perovskite structure, corner sharing of octahedral is spread over two directions^{19,20}. The zigzag layer titanates are composed of TiO_6 distorted octahedral. The position of titanium ion deviates from the center of gravity of surrounding oxygen ions and so gives rise to a dipole moment²¹. The zigzag layer of $\text{Na}_2\text{Ti}_3\text{O}_7$ has been shown to exhibit three dipole moments²¹, 5.0, 5.8, 6.2D. EPR and electrical studies in layered $\text{Na}_{1.9}\text{Li}_{0.1}\text{Ti}_3\text{O}_7$ and its copper and manganese doped derivatives have been reported by Pal *et al*^{22, 23}. The compounds $\text{Na}_2\text{Ti}_3\text{O}_7$ and $\text{Na}_2\text{Ti}_6\text{O}_{13}$ were synthesized by sol-gel method in order to obtain pure phases. Different heat-treatments were applied on powders and pellets of these materials. The effects were studied by XRD, dilatometer, TGA-DTA, SEM and electrochemical impedance spectroscopy³². The electrical conductivity and dielectric measurements in Au^+ doped/undoped KDP crystals with KCl and NaCl as additives have been reported by Ananda Kumari *et al*³⁴. The conduction mechanism in potassium borovanadate iron glass has been reported by Harshvadan R. Panchal *et al*³⁵.

No attempt has been made to characterize through EPR, dielectric-spectroscopic and conductivity studies for lithium substituted $\text{Na}_2\text{Ti}_3\text{O}_7$. Lithium ion-based

materials are found to possess increasing importance due to their potential application in high-energy batteries, as solid electrolytes and electrodes, chemical sensors and other electrochemical devices. Safety and recharge-ability problems associated to the use of metallic lithium have so far precluded their wide spread marketing that is why we have taken very small amount of lithium.

2 Experimental Details

The ceramic sample of $\text{Na}_{1.9}\text{Li}_{0.1}\text{Ti}_3\text{O}_7$ (denoted as SLT) was prepared by grinding mechanically a mixture of Na_2CO_3 (99.9% pure AR grade Merck Germany), Li_2CO_3 (99.9% pure AR grade Merck Germany) and TiO_2 powders (99% pure AR grade Merck Germany) in the stoichiometric ratio to achieve fine and homogeneous powder. The powder was heated up to 1073K for 16 h then cooled to room temperature (RT) and grinded mechanically again for an hour to achieve fine powder. The powder thus obtained was compressed at 15 MPa to get cylindrical pellets (10.25 mm in diameter and 1.2 mm in thickness). The pellets so obtained were covered with the remaining powder and heated again at 1073 K for 16 h.

The XRD pattern of SLT was collected on Iso-Debyeflex 2002, Richseifert & Co. using Cu-K α radiation generated at 30 kV and 20 mA. The formation of this titanate is confirmed by the XRD pattern obtained at room temperature.

The EPR spectra have been recorded on a Varian E-line Century Series Spectrometer E-109 operating at X-band frequencies (~ 9.3 GHz). The spectrum has been recorded on the sliced pellets of doped derivatives filled in a quartz tube of 6mm outer diameter. To get the first derivative of EPR signals, 100 kHz field modulation was used. The magnetic field was calibrated accurately with a Varian E-500 digital nuclear magnetic resonance gauss meter. The Varian temperature controller (E-257/WL-257) was used to maintain the desired sample temperature from 88 to 573K for a sustained length of time with an accuracy of about 0.5K. However, the actual temperature of the sample is measured with the help of a potentiometer using a copper constantan thermocouple junction at the sample site.

The flat faces of the sintered pellets were painted with an air-dried high purity silver paste and then mounted in the sample holder evacuated up to 10^{-3} mbar for the electrical measurements. The loss tangent ($\tan\delta$) and parallel capacitance (C_p) of the pellet-

ized samples were directly measured as a function of temperature and frequency by the HP 4194A impedance analyzer. The relative permittivity (ϵ'_r) and the bulk *ac* conductivity (σ) of the samples were calculated by using the expressions:

$$\begin{aligned} \text{Dielectric constant (real)} \quad \epsilon'_r &= C_p/C_0 \\ \text{Conductance} \quad G &= \omega C_p \tan\delta; \text{ where } \omega = 2\pi f \\ \text{Conductivity} \quad \sigma &= G(t/A) \quad \dots (1) \end{aligned}$$

where f is the frequency of *ac* signal, t the thickness and A is the area of cross-section of the pellet.

3 Results and Discussion

The EPR spectrum shown in Fig. 1 of lithium substituted compound confirms the presence of Ti^{3+} ions, which result by the reduction of Ti^{4+} ions upon lithium. The g factor is 2.679 and falls in the range characteristic of d^1 ions in the distorted octahedral site. The absence of resolved hyperfine structure expected for the two titanium isotopes ^{47}Ti (7.75% abundant, $I = 5/2$) and ^{49}Ti (5.5% abundant, $I = 7/2$) with the nuclear magnetic moment suggests that the unpaired spin is shared by several Ti nuclei³¹. The substitution of lithium ions in the interlayer space does not affect the crystal structure of $\text{Na}_2\text{Ti}_3\text{O}_7$. This confirms the presence of small lithium ions with large sodium ions in the interlayer space. The crystal structure of $\text{Na}_{1.9}\text{Li}_{0.1}\text{Ti}_3\text{O}_7$ is shown in Fig. 2, which indicates that lithium atoms are accommodated with sodium atoms in widely opened interlayer space. The unit cell is shown by dotted lines.

Fig. 3 shows the dependence of loss tangent ($\tan\delta$) on temperature in the temperature range 373-773K at some fixed frequencies for SLT. From these plots, it can be seen that the value of dielectric constant ($\tan\delta$) remains invariant with rise in temperature up to 523K for all lithium substituted sodium trititanates. The

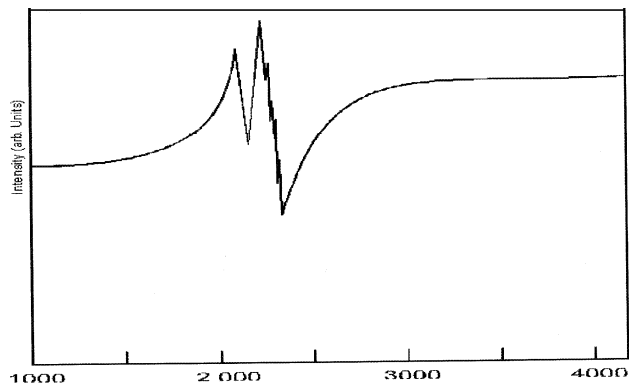


Fig. 1—EPR spectrum of lithium mixed sodium trititanates ($\text{Na}_2\text{Ti}_3\text{O}_7$)

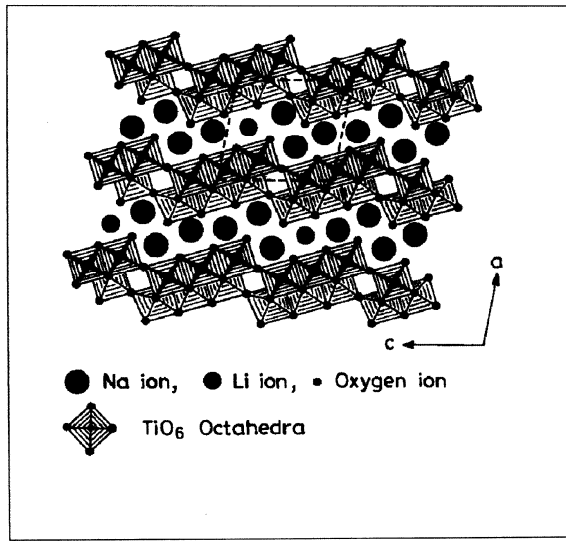


Fig. 2—Schematic structural modal for Na_{1.9}Li_{0.1}Ti₃O₇ The unit cell is shown by dotted lines

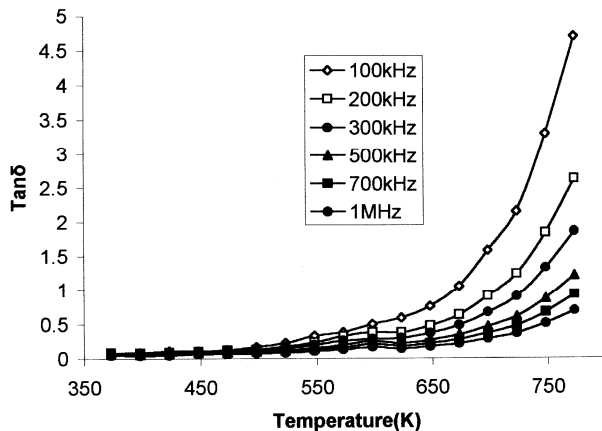


Fig. 3—Loss tangent (tanδ) versus temperature for SLT

rapid increase of dielectric loss at higher temperature in low frequency region may be due to space charge polarization. The increase of dielectric loss may be due to space charge polarization²⁴ which can be explained by using Shockley-Read mechanism²⁵. For low and middle order frequencies and at high temperatures, the impurities ions in the bulk crystal matrices capture the surface electron, causing the surface charge polarization at the surface. The electron capture process increases with the increase in temperature. The general increase of tanδ with temperature can be explained by assuming that the number of ions that takes part in relaxation polarization continuously grows with rise in temperature^{27,28}.

Fig. 4 shows the variation of dielectric constant (ϵ') with respect to temperature at some fixed frequencies

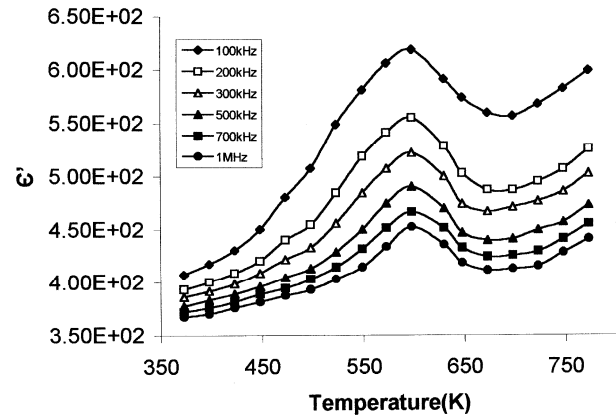


Fig. 4—Dielectric constant (ϵ') versus temperature for SLT

for SLT. It can be seen that dielectric constant (ϵ') slightly increases for SLT up to the temperature 473K then a broad peak appears at 598K then finally increases with the rise in temperature. The remaining variation of all the curves can be easily explained by proposing that the dipoles are not aligned in the low temperature region so when the temperature raises the orientation of dipoles is facilitated and this increases dielectric constant. As the temperature grows, the chaotic thermal oscillation of molecules are intensified and degree of orderliness of their orientation is diminished. This causes the curves of dependence of dielectric constant to pass through the maximum and then drop. From these plots, it is also clear that dielectric constant also increases as lithium substitution increases. The observed dispersion in the dielectric constant-temperature relation can be explained on the basis of Maxwell-Wagner model³⁶ in which the solid is assumed as composed of well conducting grains separated by the poorly conducting grain boundary. In case of SLT dispersion can be explained on the basis of that the available Ti ions on the octahedral sites give rise polarization to the maximum possible extent at low frequencies. As the applied frequency is increased, the polarized Ti ions in the titanate material could not follow the alternating field and a lag in orientation polarization arise lead to increase in dielectric constant. Fig. 5 shows the plots of $\ln\sigma T$ versus $1000/T$ at some fixed frequencies. Four regions have been identified in SLT.

Region I—The region I exist up to 473K for SLT with a peak α_1 at 448K. In this region, the trend of variations of *ac* conductivity is highly frequency dependent and temperature independent for these compositions. The nature of *ac* conductivity can be interpreted by proposing that the electronic hopping

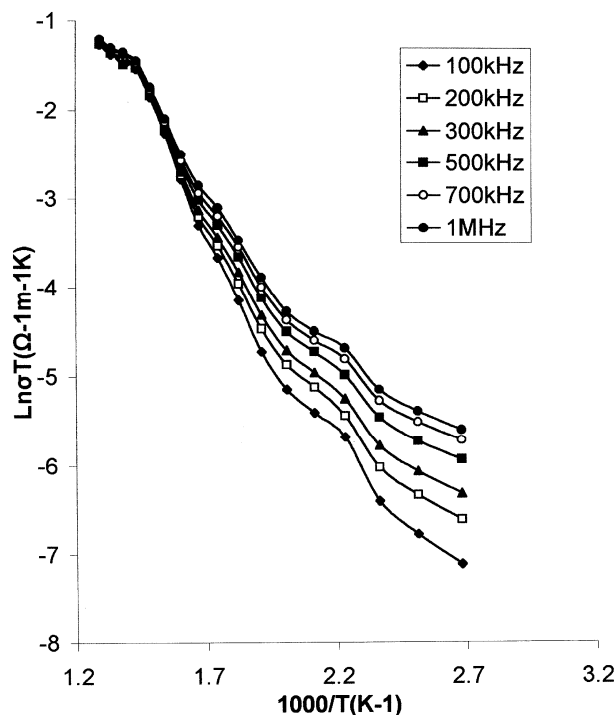


Fig. 5— $\text{Ln}\sigma T$ ($\Omega^{-1}\text{m}^{-1}\text{K}$) versus $1000/T$ (K^{-1}) for SLT

conduction, in which the hopping of electrons through shallow barrier along Ti-Ti chain take part in conduction. These electrons play a major role in this region. Such a frequency dependence of conductivity has been attributed to a wide distribution of relaxation times due to barrier height²⁷. Furthermore; it is observed that the value of *dc* conductivity²³ is lower than *ac* conductivity. This behaviour can be explained by the expression $\sigma(\omega) = A\omega^s$, where *s* is less than unity and parameter *A* shows little dependence on temperature²⁸. The appearance of peak α_1 may be due the presence of Li^+ in the interlayer space results such type of Na-Li-Ti configuration, which appreciably increases the number of loose electrons form $\text{Ti}_3\text{O}_7^{2-}$ groups. This region is very identical with those reported in conductivity plots of vacuum deposited ZnPc and CoPc thin film³². The conduction mechanism for the low temperature region can expressed³³ as:

$$\sigma = \sigma_0 \exp[(-T_0/T)^{1/4}] \quad \dots (1)$$

Region II—This region exists up to 598K for SLT. In this region, *ac* conductivity is frequency and temperature dependent and having higher slope than region I. This can be explained by assuming that the interlayer ionic conduction dominates over electronic hopping conduction. The slope of conductivity plots is

higher than region I so the mechanism of conduction may be attributed due to associated interlayer ionic conduction.

Region III—This region exists up to 698K for SLT. In this region the *ac* conductivity is temperature dependent and frequency independent for SLT. This may be due to dissociation of aggregation of Na^+ and Li^+ ions in the interlayer space, which then take part in conduction.

Region IV -This exists from 698K for SLT. In this region the *ac* conductivity is temperature dependent and frequency independent. From these plots, it is clear that modified interlayer ionic conduction exists in this region, the modification being affected by loose oxygen atoms from $\text{Ti}_3\text{O}_7^{2-}$ groups.

4 Conclusions

For first time-layered polycrystalline $\text{Na}_{1.9}\text{Li}_{0.1}\text{Ti}_3\text{O}_7$ ceramic has been synthesized and characterized through EPR, dielectric spectroscopic and *ac* conductivity studies. The possible ferroelectric phase transitions at 598K indicating ferroelectric behaviour for all compositions have been identified. Layered sodium lithium trititanates $\text{Na}_{1.9}\text{Li}_{0.1}\text{Ti}_3\text{O}_7$ ceramic can be put in the class of mixed ionic-electronic materials. The EPR spectrum of $\text{Na}_{1.9}\text{Li}_{0.1}\text{Ti}_3\text{O}_7$ confirms the partial reduction of Ti^{4+} ions to Ti^{3+} .

Acknowledgement

Author acknowledges the Department of Science and Technology (DST), Ministry of Science and Technology, Government of India, for the financial support. Thanks are also due to Dr S D Pandey, Ex-Head, Department of Physics, PPN College, Kanpur for helpful discussion.

References

- 1 Zanle H, *J Phys: Condensed Matter*, (2001) 7679.
- 2 Chen Q, Zhou W, Du G H & Peng L M, *J Advanced Mater*, 14 (2002) 1208.
- 3 Anderson S & Wadsley A D, *Acta Cryst*, 14 (1961) 1245.
- 4 Shripal & Pandey S D, *Solid State Commun*, 69 (1989) 1203.
- 5 Carlone E Bamberger & George M Begum, *J Amer Ceram Soc*, 70 (1987) 48.
- 6 Fomina L N, Neumin A D, Paluev S F, Vakarin S V & Palksin S V, *J Inorg Mat*, 30 (2001) 979.
- 7 Range K J, Fisher H, Ketterl F & Afr S, *J Chem*, 40 (1987) 233.
- 8 Wadsley A D & Mumme W G, *Acta Cryst*, VB24 (1968) 392.
- 9 Anderson S & Wadsley A D, *J Acta Cryst*, 15 (1962) 1245.
- 10 Dion M, Piffard Y & Tournoux M, *J Inorg Nucl Chem*, 40

- (1978) 917.
- 11 Batygin V G & Khimii Zh Neorgan, *Russion J Inorg Chem*, 12 (1967) 1442.
 - 12 Bouaziz R & Mayer M, *J Compt Rend Acad Sci*, 272C, (1971) 1874.
 - 13 Nalbandyan V B, Shukaev I L & Khimii Zh Neorgan, *Russian J Inorg Chem*, 35 (1990) 1085.
 - 14 Kissen J, Hoppe R & Allgem Z Anorg, *J Chem*, 582 (1990) 103.
 - 15 Nalbandyan V B, (Abstract published in EPDIC-6 Budapest, Hungary, Aug 22-25,1998) 233.
 - 16 Yakubovich O V & Kireev V V, *Crystallography Report* 48, No 1 (2003) 24.
 - 17 Shripal, Badhwar Sugandha, Maurya Deepam, Kumar Jitendra & Tandon R P, Proceeding of ACMP-05 (Allied Publisher, 11-12 Feb2005) p250.
 - 18 Shripal, Badhwar Sugandha, Maurya Deepam, Tandon R P & Kumar Jitendra, *J Mater Sci, Materials in Electronics*, 16 (2005) 495.
 - 19 Rao C N R & Ravean B, *Transition Metal Oxides*, (VCH Publishers) (1995) 103.
 - 20 Wells A F, *Structural Inorganic Chemistry*, Oxford Univ Press (1984) 218.
 - 21 Ogera S, Sato K & Inoue Y, *J Phys Chem*, 2 (2000) 2449.
 - 22 Pal D, Chand Prem, Tandon R P & Shripal: *J Korean Chem Soc*, 49 (2005) 560.
 - 23 Pal D, Chand Prem & Shripal, Proceeding of NSFD-XIII, (Allied Publisher 23-25 Nov 2004) 39.
 - 24 Das B P, Choudhary R N P & Mahapatra P K, *J Mats Sci & Engg B*, 104 (2003) 105.
 - 25 Bogoroditsky N P, Pasyukov V V & Tareev B, *Elect Engg Mater* (Mir Publisher Moscow), 1979, 65.
 - 26 Mansingh Abhai, Tandon R P & Vaid J K, *Phys Rev B*, 21 (1980) 5829.
 - 27 G E Pike, *Phys Rev B*, 6 (1972) 1571.
 - 28 Lingwal Vijendra, Semwal B S & Panwar N S, *Bull Mater Sci*, 26 (2003) 619.
 - 29 Yueming Li, Wen Chen, Jing Zhou, Qing Xu, Huajun Sun & Meisong Liao, *Ceramic International*, 31 (2005) 139.
 - 30 Sauvet A-L, Baliteau S, Lopez C & Fabry P, *J Solid State Chem*, 177 (2004) 4508.
 - 31 Abragam A & Bleaney B, *Electron paramagnetic resonance of transition ions*, (Clarendon Press, Oxford) 1970.
 - 32 Rajesh K R & Menon C S, *Indian J Pure & Appl Phys*, 43 (2005) 964.
 - 33 Shklovskii B I & Efros A L, *Electronic properties of doped semiconductors* (Springer, Berlin), 1984.
 - 34 Kumari R A & Chandramani R, *Indian J Pure & Appl Phys*, 43 (2005) 123.
 - 35 Panchal H R & Kanchan D K, *Indian J Pure & Appl Phys*, 43 (2005) 137.
 - 36 Volgar J, *Prog Semicond*, 4 (1960) 207.